ELSEVIER

Catalysis Today 63 (2000) 197–207

CATALYSIS TODAY

www.elsevier.com/locate/cattod

Factors controlling the selectivity of V_2O_5 supported catalysts in the oxidative dehydrogenation of propane

Gianmario Martra [a,*], Franco Arena [b,c], Salvatore Coluccia [a], Franco Frusteri [c], Adolfo Parmaliana [c,d]

[a] *Dipartimento di Chimica IFM, Universita' di Torino, Via P. Giuria 7, I-10125 Torino, Italy*
[b] *Dipartimento di Chimica Industriale, Universita' di Messina, Salita Sperone c.p. 29, I-98166 S. Agata (Messina), Italy*
[c] *Istituto CNR-TAE, Salita S. Lucia 39, I-98126 S. Lucia (Messina), Italy*
[d] *Dipartimento di Chimica, Universita' "La Sapienza", P.le A. Moro 5, I-00185 Roma, Italy*

Abstract

The surface properties of a series of V_2O_5 catalysts supported on different oxides (Al_2O_3, H–Na/Y zeolite, MgO, SiO_2, TiO_2 and ZrO_2) were investigated by transmission electron microscopy and FTIR spectroscopy augmented by CO and NH_3 adsorption. In the case of the V_2O_5/SiO_2 system TEM images evidenced the presence of V_2O_5 crystallites, whereas such segregated phase was not observed for the other samples. VO_x species resulted widely spread on the surface of Al_2O_3, H–Na/Y zeolite, MgO and SiO_2, whereas on TiO_2 and ZrO_2 they are assembled in a layer covering almost completely the support. Furthermore, evidences for the presence in this layer of V–OH Brønsted acid sites close to the active centres were found. It is proposed that propene molecules primarily produced by oxydehydrogenation of propane can be adsorbed on this acid centres and then undergo an overoxidation by reaction with redox centres in the neighbourhood. This features could account for the low selectivity of V_2O_5/TiO_2 and V_2O_5/ZrO_2 catalysts.

Keywords: V_2O_5; Supported catalysts; TEM; FTIR; ODH of propane

1. Introduction

Catalytic oxidation is a very important feature in modern chemical industry, and selective oxidation catalyst play a central role in the processes devoted to the functionalization of alkenes and aromatics, which are widely obtained from petroleum. However, the interest of petrochemical industry towards the use of alkanes is growing up, as they are even more economical, readily available raw materials, with low toxicity as compared to aromatics.

Furthermore, the olefins obtained by steam cracking of naphtha and from fluid catalytic cracking in oil refining are not sufficient for meeting the actual demand and growth rate. Consequently, the increased future demand for olefins will be likely satisfied mainly by direct production in dedicated plants. In this frame the dehydrogenation of propane to propylene, a very large scale chemical mainly obtained from oil at present, appears as an attractive process. However, the dehydrogenation of paraffins to give the corresponding olefins and H_2 is a strongly endothermic process occurring at temperature above 873 K, which favour other unwanted reactions. An effective alternative is the oxidative dehydrogenation (ODH) process, since it could allow to overcome technological and chemical draw-

* Corresponding author. Tel.: +39-11-670-7538; fax: +39-11-670-7855.
E-mail address: martra@ch.unito.it (G. Martra).

0920-5861/00/$ – see front matter
PII: S0920-5861(00)00460-0

backs associated with pure dehydrogenation processes.

Vanadia supported catalysts are used in almost all processes devoted to the selective oxidation of alkanes, and they behave as effective systems also for the ODH of paraffins, as widely reported in a relevant number of papers and reviews [1–6]. A number of factors influence the catalytic behaviour of such catalysts, as the nature, structure and the dispersion of the supported species, the nature of the support, the presence of additives (often present on oxide carriers of pigment grade). In particular, some features of the catalytic pattern of vanadia supported catalysts in dependence on the size of paraffin molecules in the feed suggested that the degree of dispersion (distance) of the active sites can influence the selectivity towards olefins in ODH reactions [3,5]. Furthermore, olefins produced in such processes are better preserved from further oxidation if basic centres are present on the catalyst surface, as they facilitate the desorption of alkenes, more basic compounds than the corresponding alkanes [1–6]. By contrast, the presence of Brønsted and/or Lewis acid sites plays a detrimental role, decreasing the rate of desorption of olefins from the catalyst.

In this frame, a systematic study of a series of supported catalysts intended for the oxydehydrogenation of propane has been carried out [7–9], enlightening that the reactivity of these systems is controlled by their redox properties and that the reducibility of the supported species is affected by both redox and acid–base properties of the support [8,9].

In this paper further studies on the dispersion of the supported species and on their structure and nature, carried out by using transmission electron microscopy and FTIR spectroscopy augmented by the adsorption of probe molecules, are reported.

2. Experimental

2.1. Materials

Supported V_2O_5 catalysts were prepared by incipient wetness of commercial oxide (Al_2O_3, H–Na/Y zeolite, MgO, SiO_2, TiO_2, and ZrO_2) carriers with an aqueous solution (pH = 11) of ammonium metavanadate. All samples were dried at 383 K and then calcined in air at 873 K for 14 h. The final loading was in the 4.7–5.3 wt.% V_2O_5 range. The list of oxides used as support and of the supported catalysts, along with their notation and loading, specific surface area (SSA_{BET}) and theoretical distribution of vanadium atoms on the surface are reported in Table 1.

High purity CO and NH_3 (Matheson) were employed in the spectroscopic measurements. CO was used without any further purification except liquid nitrogen trapping, while NH_3 was purified through several freeze–pump–thaw cycles.

2.2. Methods

Catalytic test. The POD reaction was carried out in a flow quartz microreactor connected on line with a GC equipped with a three-column analytical system. The activity of catalysts has been evaluated at T_R = 773 K and P_R = 1 bar using a catalyst mass sample of 0.01–0.25 g (diluted (1/10, w/w) with SiC) and a reaction mixture having the molar composition

Table 1
List of the oxides used as support and of the V_2O_5 supported catalysts, reporting their code, loading (wt.% V_2O_5), surface area (SSA_{BET}) and theoretic surface V distribution (VO_x nm^{-2})

Supports		Catalysts				
Sample	SSA_{BET} ($m^2\,g^{-1}$)	Sample	Code	V_2O_5 (wt.%)	SSA_{BET} ($m^2\,g^{-1}$)	VO_x (nm^{-2})
H–NaY	632	V_2O_5/(H–Na/Y)	VY	5.3	350	1.00
SiO_2	381	V_2O_5/SiO_2	VS	5.0	286	1.16
Al_2O_3	185	V_2O_5/Al_2O_3	VA	4.8	209	1.52
MgO	24	V_2O_5/MgO	VM	4.7	101	3.08
TiO_2	51	V_2O_5/TiO_2	VT	5.0	41	8.07
ZrO_2	37	V_2O_5/ZrO_2	VZ	5.3	34	10.32

C_3H_8:O_2:N_2:He = 2:1:1:8 flowing at the rate of 100 STP $cm^3\,min^{-1}$. Further details are reported in Ref. [7].

High resolution transmission electron microscopy (HRTEM). Electron micrographs of the samples were obtained with a Jeol 2000EX instrument equipped with polar piece and top entry stage. The samples were ultrasonically dispersed in *n*-exane, and a drop of the obtained suspension put on a Cu grid covered with a lacey carbon film.

FTIR spectroscopy. For FTIR measurements, the samples were pressed in the form of self-supporting pellets and placed in a quartz cell with KBr windows allowing measurement both at room temperature (r.t.) and liquid nitrogen temperature, permanently attached to a conventional vacuum line (residual pressure: 1×10^{-6} Torr, 1 Torr = 133.33 N m^{-2}) allowing all thermal and adsorption–desorption experiments to be carried out in situ. Before recording the spectra, the samples were dehydrated by outgassing at 773 K for 1 h. As this treatment is known to promote the reduction of V^{5+} ions to lower oxidation states, the samples were subsequently re-oxidised by heating in 100 Torr O_2 for 1 h at the same temperature, cooled to room temperature under oxygen and then pumped off for 1 h. The spectra were collected with a Bruker IFS 48 instrument (resolution: 4 cm^{-1}). Their intensity was normalised with respect to the apparent "density" (mg cm^{-2}) of the pellets.

3. Results and discussion

3.1. Preliminary remarks: catalytic activity and coordinative state of V^{5+} ions

Table 2 reports the activity of the various catalysts in the oxidative dehydrogenation of propane at 773 K. It can be noticed that the distribution of C_3H_6 selectivity appears quite large (ca. 30–70%) with respect to the comparatively small range of C_3H_8 conversion (ca. 2–5%). However, if the specific surface activity is taken into account, VT and VZ exhibit the highest activity by far and low C_3H_6 selectivity (Table 2, entries 5 and 6). VS and VA are characterised by a low specific activity, which is accompanied by a high C_3H_6 selectivity (Table 2, entries 2 and 3), while VH and VM, which exhibit a low specific activity, behave as poor selective catalysts (Table 2, entries 1 and 4). In previous works [8,9] it was put in evidence that the most active catalysts exhibited the lowest onset temperature of reduction in temperature programmed reduction (TPR) measurements, indicating that the reactivity of the supported species in POD is controlled by their redox properties.

Table 2
Oxidative dehydrogenation of propane on the various V_2O_5 supported catalysts at 773 K reported in terms of C_3H_8 conversion, C_3H_6 selectivity ($S_{C_3H_6}$) and specific surface activity (SSA)

Entry	Catalyst	C_3H_8 conversion (%)	$S_{C_3H_6}$ (%)	SSA ($nmol_{C_3H_8}\,m^{-2}\,s^{-1}$)
1	VH	4.4	38	34.2
2	VS	3.3	72	12.6
3	VA	3.2	73	104.0
4	VM	4.2	31	46.4
5	VT	5.1	30	1690.0
6	VZ	2.5	46	1000.0

Furthermore, DR UV–Vis data evidenced that essentially V^{5+} ions, which were the overwhelming species after dehydration/oxidation at high temperature, belonged to different types of structures with different coordination states in dependence on the oxide support [9]. Namely, V^{5+} ions in pseudo-tetrahedral coordination isolated or clusterised in oligomeric structure were found in the VY, VS, VA and VM catalysts, whereas the presence of V^{5+} centres in a square-pyramidal coordination forming two-dimensional layers were inferred in the case of the VZ and VT systems. Finally, evidences for minor fraction of three-dimensional V_2O_5 like structure were obtained for VS, VT and VZ catalysts.

These data indicated that significant differences in the nature and dispersion of the supported species occurred among the catalyst series, and this, as pointed out in Section 1, could influence the catalytic performance of the various systems also. Thus, further investigations devoted to obtain information about the actual structure of the supported phase were carried out.

3.2. Dispersion on the VO_x species on the support

3.2.1. HRTEM study

Owing to the low specific surface area of the TiO_2 and ZrO_2 used as support, the theoretical distribution

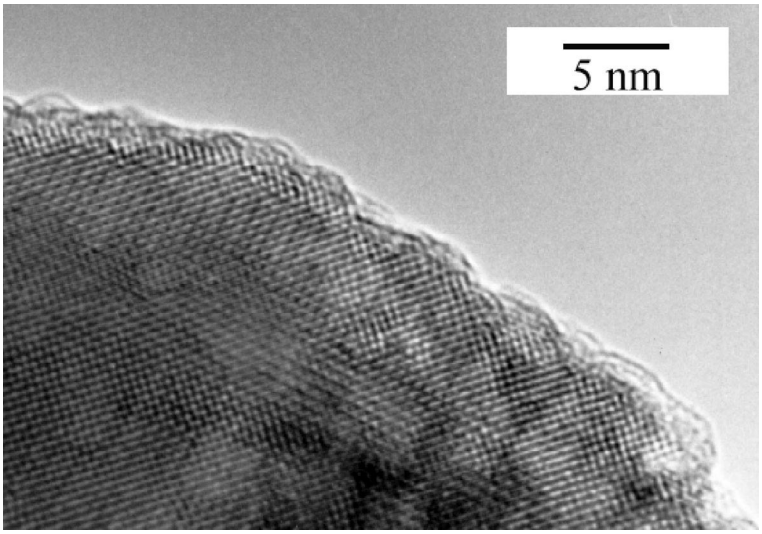

Fig. 1. High resolution transmission electron micrograph of the V_2O_5/TiO_2 catalyst. Original magnification: 1 000 000×.

of vanadium atoms on the surface of VT and VZ catalysts resulted quite high (Table 1), close to the monolayer surface coverage (i.e. 7–8 VO_x nm^{-2} [10]) in the case of VT, or even higher for VZ. To check the dispersion of the supported phase HRTEM studies were then carried out. High resolution images of the VT system showed that catalyst microcrystals, the bulk of which produced series of regularly spaced fringes related to the crystallographic planes of anatase, are covered by an almost continuous thin layer exhibiting an amorphous habit (Fig. 1). Neither multilayer two-dimensional patches nor three-dimensional particles due to a V_2O_5-like phase were observed. It was difficult to recognise in the amorphous layer the actual presence of vanadium atoms. A similar thin amorphous film was observed in parallel experiments on the bare TiO_2, likely generated by the interaction of the electron beam with the material and/or the decomposition under the electron beam of some residual of the organic liquid used to suspend the powder during the preparation of the sample. The similarity between the images of the bare TiO_2 and the VT system indicated that V^{5+} species are well dispersed on the support.

Similar features were observed in the case of the VZ system, without significant differences between the images of the bare ZrO_2 support (micrographs not reported). No segregated V_2O_5 particles were observed, although the VO_x content exceeded the monolayer capacity. It can be proposed than a few multilayers on the surface of the support or very small vanadia particles, both not easily distinguishable on the ZrO_2 microcrystals, can be present.

No evidences for agglomerated forms of the supported phase were obtained for VA, VM and VY catalysts, whereas large V_2O_5 crystallites were detected in the VS sample, well separated from the support (Fig. 2). TPR measurements indicated that ca. 20% of the V^{5+} ions are present in such form [11]. This result well agrees with literature data, widely reporting that, due to the acidic character of both silica and vanadia, a quite low amount of VO_x species is retained in a dispersed form on the SiO_2 surface [12].

3.2.2. FTIR spectra of the surface hydroxyl groups and of CO adsorbed at 77 K

Insights on the actual distribution of the supported phase on the surface of the carriers were obtained for all catalysts by comparing the IR spectra of the bare supports in the 3800–3000 cm^{-1} range with those of the corresponding supported systems. In that region bands due to the stretching mode of hydroxyl groups typical of the various bare oxides were observed (Fig. 3, curves a′–f′). A discussion of the features of such bands is outside the scope of this

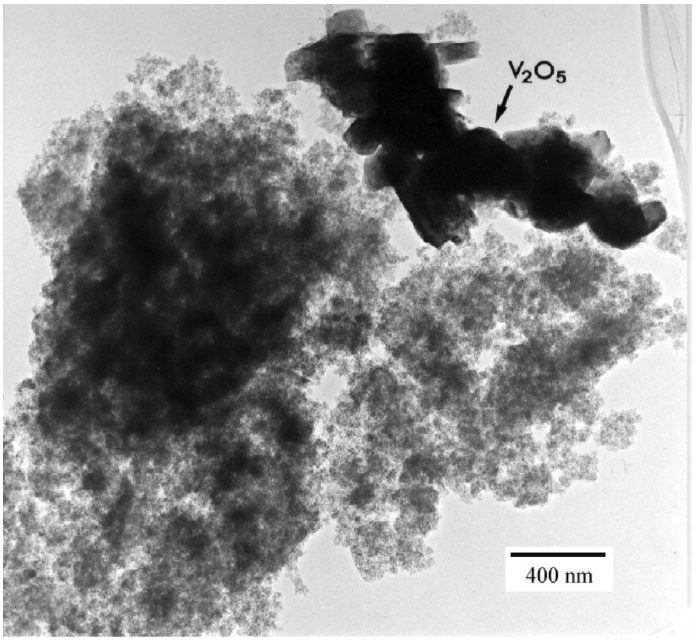

Fig. 2. Transmission electron micrograph of the V_2O_5/SiO_2 catalyst. Original magnification: 15 000×.

work, and details can be found in the rich literature related to this subject ([13] for HY; [14] for SiO_2; [15] for Al_2O_3; [16] for MgO; [17] for TiO_2 and [18] for ZrO_2). However, it can be noticed that the spectrum of the HY support (Fig. 3, curve a) exhibits a different pattern of the relative intensity of the various components with respect to usual Brønsted acidic faujasites, with a predominance of the band at 3740 cm^{-1}, due to silanols groups, on the components in the 3700–3500 cm^{-1} range, due to Brønsted acidic protons. This feature should be related to the treatment with HCl carried out on the parent NaY to introduce acidic protons in the zeolitic structure, resulting in the production of defects in the silicate

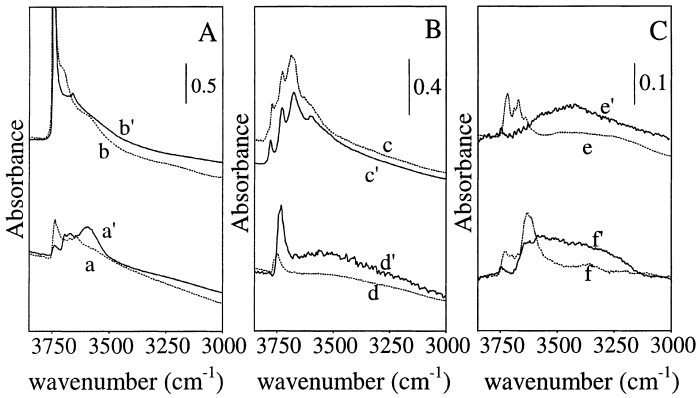

Fig. 3. IR spectra in the 3850–3000 cm^{-1} range of the bare oxide carriers and of the corresponding V_2O_5 supported catalysts outgassed and re-oxidised at 773 K for 1 h (see Section 2): (a) H–Na/Y zeolite, (a′) VY; (b) SiO_2, (b′) VS; (c) Al_2O_3, (c′) VA; (d) MgO, (d′) VM; (e) TiO_2, (e′) VT; and (f) ZrO_2, (f′) VT.

framework. The dispersion of vanadia species in this matrix results in the decrease in intensity of the peak at 3740 cm^{-1}, indicating that silanols were consumed to anchor the supported species and/or perturbed by them, and complex changes occurred in the region at low frequency, suggesting that original Brønsted acid protons are partially involved in the dispersion of the supported phase and that, likely, new ones are produced (Fig. 3, curve a′).

In the case of the VS sample, only a limited decrease in intensity of the complex band in the 3750–3300 cm^{-1} range, due to silanols groups, in comparison with the bare SiO_2 was observed (Fig. 5, curves b and b′). This indicated that only a small fraction of the surface of silica was covered by the supported species. Noticeably, a weak, but well defined peak appeared at 3658 cm^{-1} in the spectrum of the VS catalyst, which can be assigned to V–OH Brønsted acidic centres [19].

Limited changes in the spectral pattern related to the hydroxyl groups resulted from the comparison of the spectra of bare Al_2O_3 (Fig. 3, curve c) and VA catalyst (Fig. 3, curve c′) indicating that also in this case only a small fraction of the support was covered by the vanadia phase. The new, weak component observed at 3620 cm^{-1} in the spectrum of VA (Fig. 3, curve c′) could be due to V–OH Brønsted acidic centres.

By contrast, a significant increase in intensity of the absorptions due to hydroxyl groups of the support were observed passing from bare MgO (Fig. 3, curve d) to the VM system (Fig. 3, curve d′), while no bands due to V–OH species were detected. BET measurements indicated that the specific surface area (SSA_{BET}) of the V_2O_5/MgO sample is significantly higher than that of the bare MgO carrier (see Table 1). This should be a consequence of the hydration of the MgO surface layers occurring during the impregnation with the solution of ammonium metavanadate. As reported for highly regular MgO microcubelets exposed to water [20], the contact with an aqueous medium results in a deep modification of the morphology of the microcrystals of MgO. In this case extensive hydration to $Mg(OH)_2$ and subsequent dehydration to MgO account for the significant increase of the specific surface area. Under these circumstances mixed magnesia–vanadia phases may well be produced, possibly with part of the vanadium centres covered by MgO layers.

Marked differences were observed between the spectra of bare TiO_2 and VT catalyst. In fact, the 3760–3560 cm^{-1} spectral pattern due to hydroxyl groups on the surface of TiO_2 (Fig. 3, curve e) was completely absent in the spectrum of the VT sample, where a broad and ill defined absorption in the 3600–3100 cm^{-1} was observed (Fig. 3, curve e′). Similarly, the original bands due to hydroxyl groups on the surface of ZrO_2 (Fig. 3, curve f) resulted completely depleted in the spectrum of the VZ sample, while a new broad feature in the 3600–3100 cm^{-1} range appeared (Fig. 3, curve f′). These results suggested that in both cases large fractions of the surface of TiO_2 and ZrO_2 supports are covered by the supported phase.

However, as a consequence of the dehydration/reoxidation treatment at 773 K the surface of TiO_2, ZrO_2 and corresponding supported catalysts should be largely dehydroxylated, and then the results just commented allowed to monitor only the portion of the surface of the various samples where hydroxyl groups were left. To obtain insights on the distribution of the VO_x species on the other part of the surface of these systems, FTIR spectra of CO adsorbed at 77 K were recorded.

The admission of CO at 77 K on bare TiO_2 produced sharp peak at 2177 cm^{-1} and a weaker and broader band at 2154 cm^{-1} (Fig. 4A, curve a). The main component is assigned to CO molecules adsorbed on surface coordinatively unsaturated (cus) Ti^{4+} ions, while the second component is due to CO molecules adsorbed on the hydroxyl groups [21]. Weaker and broad features at even lower frequency should be due to liquid-like CO in micropores [22]. By decreasing the CO coverage, a progressive shift towards higher frequency of the band due to CO on Ti^{4+} ions occurred (Fig. 4A, curves b–s), owing to the progressive vanishing of the dynamic and static adsorbate–adsorbate interactions as the amount of adsorbed CO decreases [21]. By contrast, in the spectrum of CO adsorbed on the VT catalyst, a broad and weak band at 2160 cm^{-1} was observed as main feature, with weak and poor resolved shoulders at ca. 2180 and 2155 cm^{-1}, which are vestiges of the absorptions present in the spectrum of bare TiO_2 (Fig. 4A, curves a′–m′). The component at 2160 cm^{-1} should be due to CO adsorbed on the hydroxyl groups present on the supported phase. It may be of interest that a band in this position was

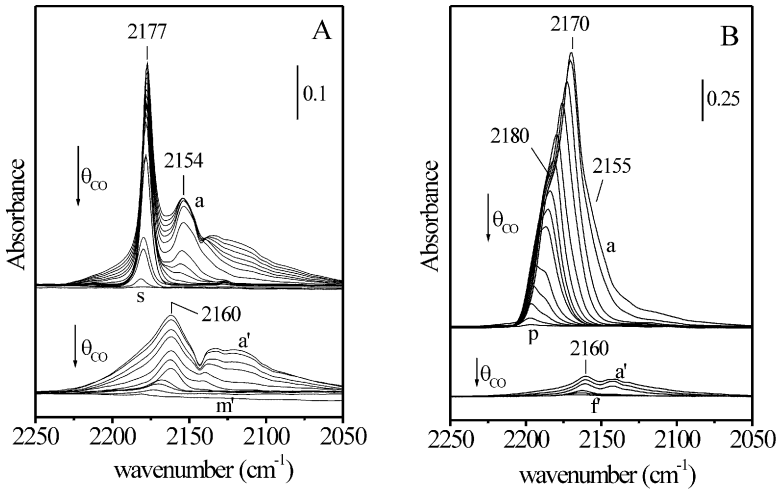

Fig. 4. IR spectra of CO adsorbed on TiO_2, VT, ZrO_2 and VZ outgassed and re-oxidised at 773 K for 1 h (see Section 2): (A) spectra recorded under decreasing CO coverage from the presence of 80 Torr CO to outgassing for 5 min at 77 K: curves (a–s) TiO_2, curves (a′–m′) VT; (B) spectra recorded under decreasing CO coverage from the presence of 80 Torr CO to outgassing for 5 min at 77 K: curves (a–s) ZrO_2, curves (a′–m′) VZ.

assigned to CO interacting with Brønsted acidic protons at the surface of a WO_3/TiO_2 catalyst [23]. This result clearly indicated that the overwhelming part of the support is covered by VO_x species, as only a very small fraction of Ti_{cus}^{4+} and hydroxyl groups of the TiO_2 surface was accessible to CO.

Similar insights resulted by comparing the ZrO_2 and VZ samples. By adsorbing CO at low temperature on ZrO_2 a peak at 2170 cm^{-1}, with shoulders at 2180 and 2155 cm^{-1}, was observed (Fig. 4B, curve a). By decreasing the amount of adsorbed CO this last component disappeared first, while the main band at 2170 cm^{-1} progressively shifted to higher frequency giving origin to two distinct components (Fig. 4B, curves b–p). Absorptions at frequency higher than 2160 cm^{-1} can be assigned to CO molecules adsorbed on two families of Zr_{cus}^{4+} ions of different Lewis acid strength, their complex evolution in dependence on the CO coverage resulting from the different structure of the adsorbed phase at various CO coverages, while the shoulder at 2155 cm^{-1} should be related to CO molecules adsorbed on surface hydroxyl groups [24,25]. None of these features were observed in the spectra of CO adsorbed on the VZ catalyst, where only a weak band at 2160 cm^{-1} was present (Fig. 4B, curves a′–f′), indicating that the support was completely covered by VO_x species. For the component at 2160 cm^{-1} the same assignment than for the analogous band observed in the spectra of the VT sample can be proposed.

The overall results of Figs. 3C, 4A and 4B indicate that in the case of VT and VZ catalysts the supported phase forms an almost continuous layer covering the surface of the oxide carrier. A network of active sites close to each other is then present, and this could influence the catalytic pattern of these systems. It is widely accepted that to avoid the reaction of overoxidation of the primary product of alkane conversion, it is necessary that the adsorbed paraffin finds very few sites which may be active for oxidation close to the adsorption centres [3,5,26]. In the case of oxydehydrogenation processes, it was proposed that distance between active sites influence the selectivity of the ODH of *n*-butane [5], while propane, with a shorter chain of C atoms, should be less sensitive to this effect. However, the possibility that a primary product undergoes overoxidation by neighbour active sites depends also on the rate of its desorption from the catalyst surface. In the case of the production of olefins, basic sites facilitate the desorption of alkenes, which are more basic than the corresponding alkanes, whilst their desorption rate is decreased by the presence of Brønsted

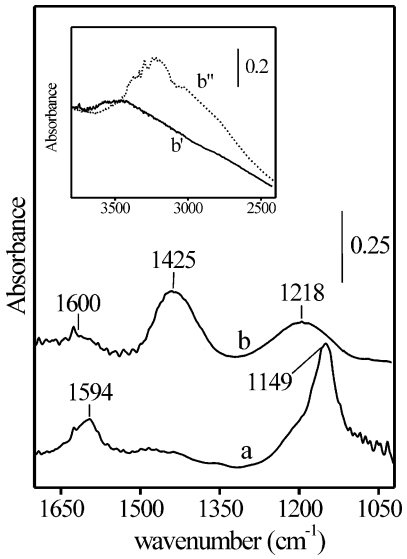

Fig. 5. IR spectra of NH_3 (20 Torr) adsorbed at room temperature on TiO_2 (curve a) and VT (curve b) outgassed and re-oxidised at 773 K for 1 h (see Section 2). The spectra are reported in absorbance, having subtracted the spectrum of the samples before adsorption of NH_3 as background. Inset: IR spectra in the 3800–2400 cm^{-1} region of (b′) VT before the adsorption of ammonia; (b″) in the presence of 20 Torr NH_3.

and/or Lewis acid sites, thus favouring their further oxidation [3,5]. This aspect was then investigated also by FTIR spectroscopy of adsorbed ammonia.

3.3. Location of Brønsted acid and redox sites: FTIR spectra of adsorbed NH_3

Oxide carriers usually exhibit only surface Lewis acid centres (i.e. coordinatively unsaturated cations, hydroxyl groups), while the dispersion on their surface of VO_x species is known to produce Brønsted acid sites [27,28]. Thus, a FTIR study of the adsorption of NH_3, a probe molecules which is highly sensitive to both Lewis and Brønsted acid centres, was carried out on the bare supports and the supported catalysts. For the sake of brevity, only the spectra of ammonia adsorbed on TiO_2–VT and ZrO_2–VZ couples will be shown.

The adsorption of ammonia on the bare TiO_2 support resulted in the appearance of bands at 1594 and 1149 cm^{-1} (Fig. 5, curve a), assigned to the asymmetric and symmetric deformation modes respectively of NH_3 molecules adsorbed on Ti^{4+} ions [29]. These components were completely absent in the spectrum of ammonia adsorbed on the VT catalyst, which appear dominated by a band at 1425 cm^{-1} with weaker components at 1650, 1600 and 1218 cm^{-1} (Fig. 5, curve b), indicating that original Ti^{4+} centres are not accessible to NH_3 molecules. This feature confirms the insights obtained by the IR spectra of hydroxyl groups (Fig. 3C, curves e′ and e) and adsorbed CO (Fig. 4A and B). The two bands at 1600 and 1218 cm^{-1} can be assigned to NH_3 molecules adsorbed on V^{5+} cations belonging to VO_x species, while the weak component at 1650 cm^{-1} and the main peak at 1425 cm^{-1} should be ascribed to the symmetric and asymmetric deformation modes, respectively, of NH_4^+ ions formed by reaction of ammonia with Brønsted acid V–OH centres [27,29–31]. As a related feature, the broad band in the 3700–3000 cm^{-1} range present in the spectrum of the VT sample (inset Fig. 5, curve b′) was depleted by the adsorption of ammonia, while an intense and complex series of band due to the stretching modes of NH_4^+ and NH_3 adsorbed species appears (Fig. 5, curve b′) [29]. Noticeably, the decrease of the amount of adsorbed species by outgassing at increasing temperature resulted in a related decrease of the spectral components due to ammonium ions, both at high and low frequency, and the restoration of the broad 3700–3000 cm^{-1} band due to hydroxyl groups, indicating that these species are V–OH groups with Brønsted acid character (spectra not reported).

Similar results were obtained for the VZ sample, but the transparency of the ZrO_2 support at low frequency allowed to obtain additional insights on the features of the Lewis and Brønsted centres. In fact, in this case a well-defined band at 1020 cm^{-1}, with a shoulder at 1031 cm^{-1}, and a broad and intense absorption at 870 cm^{-1} were observed (Fig. 6, curve a). On the basis of a recent study of V_2O_5/ZrO_2 systems [32], the component at 1020 cm^{-1} can be assigned to the V=O stretching mode of VO_x monomeric species, while absorptions at 1030 and 870 cm^{-1} should be due to the V=O and V–O–V stretching modes of polymeric $(VO_x)_n$ structures (mainly two-dimensional), respectively.

The contact with ammonia produced the depletion of the broad band in the 3650–3100 cm^{-1} range due to hydroxyl groups, and the complex patterns due to the N–H stretching modes of NH_4^+ and NH_3

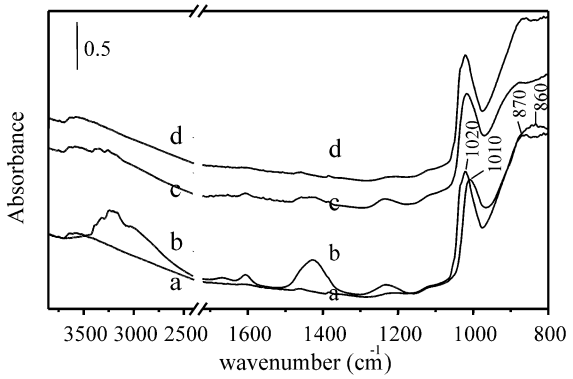

Fig. 6. IR spectra of NH_3 adsorbed at room temperature on VT catalyst outgassed and re-oxidised at 773 K for 1 h (see Section 2): (a) VT catalyst before the adsorption of ammonia; (b) in the presence of 20 Torr NH_3; (c) after outgassing at 523 K for 30 min; (d) after outgassing at 673 K for 30 min.

adsorbed species in the 3400–2500 cm^{-1} range appeared (Fig. 6, curves a and b). At the same time, a weak component at 1660 cm^{-1} and a main band at 1437 cm^{-1} due to NH_4^+ ions formed at the expenses of V–OH Brønsted acid centres and two adsorptions at 1608 and 1238 cm^{-1} due to NH_3 adsorbed on V^{5+} Lewis acid centres in VO_x species were observed (Fig. 6, curves a and b). At lower frequency, the adsorption of ammonia produced the shift of the complex band at 1020–1010 cm^{-1} and of the broad component at 870–840 cm^{-1} (Fig. 6, curves a and b).

By outgassing at 523 K the intense pattern in the 3400–2500 cm^{-1} appeared strongly reduced in intensity, while the broad band at 3650–3100 cm^{-1} was almost completely restored (Fig. 6, curve c). At lower frequency, only vestiges of the 1660 and 1437 cm^{-1} absorptions due to NH_4^+ ions was still present, and at the same time, both features at 1020 and 870 cm^{-1} were largely restored, whilst bands due to adsorbed NH_3 molecules appeared almost unchanged (Fig. 6, curve c).

Spectral features related to NH_3 molecules on Lewis acid sites disappeared after outgassing (and re-oxidation) at 673 K, and the original features were fully restored in all spectral ranges (Fig. 6, curve d). The higher stability of these adsorbed species with respect to NH_4^+ ions were observed in previous study on an industrial V_2O_5–WO_3/TiO_2 catalyst [33].

All these data clearly indicated that ammonium ions are formed by reaction with Brønsted acid V–OH groups, but at the same time they perturb some V=O and V–O–V bonds of VO_x and $(VO_x)_n$ species. It can be then proposed that that Brønsted acid sites are located in the neighbourhood of centres responsible for the redox (catalytic) activity. The presence of Brønsted acid sites in the network of the supported species should result in the absorption of the alkene molecules produced from the oxydehydrogenation of propane in a structure were several, aggregated active sites are present, and this can significantly increase the possibility that olefin molecules undergo a further oxidation. This proposal can account for the low selectivity towards propene exhibited by both VT and VZ catalysts (Table 2, entries 5 and 6).

As for the other catalysts, in the case of the SiO_2–VS and Al_2O_3–VA systems only bands due to NH_3 molecules on Lewis acid centres were observed for the bare supports, whilst bands due to NH_4^+ ions formed by reaction of ammonia with Brønsted protons were also detected for the supported catalysts. However, for both VS and VA samples the bands assigned to NH_3 molecules on the Lewis acid centres of the supports still dominated the spectrum by far.

The bare H–Na/Y zeolite contained both Lewis and Brønsted acid sites, and then the contact with of ammonia produced in the IR spectrum bands due to both NH_3 and NH_4^+ adsorbed species. A slightly higher intensity of the components due to ammonium ions was observed for the VY catalyst, indicating that also in this case the introduction of VO_x species was accompanied by the appearance of Brønsted centres.

By contrast, no bands due to NH_4^+ ions were detected for the VM sample, which simply exhibited components due to NH_3 adsorbed molecules, as for the corresponding MgO carrier.

On this basis, also the poor catalytic behaviour of the VY sample can be ascribed to the role of Brønsted acid protons, which can act as absorbing sites for propene. These centres are located in the cavities of the zeolitic structure, where the VO_x species should be hosted also. Along their path into the microporous framework before to leave the catalyst microcrystals, olefin molecules can be absorbed on acidic protons in the cavities close redox centres, and undergo further oxidation. As reported above, Brønsted acid sites were observed also for VS and VA catalysts. However, in these systems the supported phase, mainly present as isolated monomeric VO_x and oligomeric $(VO_x)_y$

species, is widely spread on the support, and then the presence of large ensembles of active sites containing also acidic protons should be less probable.

As for MV, it was proposed above that magnesium vanadate phases are produced, possibly covered by MgO overlayers, to explain the overall low activity of the system. This is accompanied by low selectivity for propene, though no Brønsted acid sites are present. Therefore, the overoxidative properties must be associated with the presence of vanadate phases active in the total oxidation of propane, the structure of which is still actively debated [34,35].

4. Conclusions

The results obtained by the investigations carried out by transmission electron microscopy and FTIR augmented by CO and NH_3 spectroscopy indicated that the dispersion, structure and relative location of surface sites of vanadia catalysts are strongly affected by the nature of the support. Oxide carriers with high specific surface area, as H–Na/Y zeolite, SiO_2 and Al_2O_3 allowed a high dispersion of the VO_x species, which cover only a limited part of the support. In the case of MgO, the occurrence of a partial dissolution/re-precipitation of the oxide matrix results in the incorporation of a fraction of V^{5+} ions in the bulk of the catalyst.

By loading TiO_2 and ZrO_2 of low specific surface area with an amount of VO_x species close to the monolayer capacity, a layer of VO_x species which cover almost completely the support was obtained. In such condition, a close proximity of active centres can be suggested.

For all catalyst, except that supported on MgO, V–OH Brønsted acid groups are formed as a consequence of the dispersion of VO_x species. The results obtained by FTIR spectroscopy of adsorbed ammonia on the VZ catalyst indicated that V–OH Brønsted centres are located in the neighbourhood of species bearing V^{5+}ions involved in V=O and V–O–V bonds, which are usually considered as the catalytic active species. Propene molecules primarily produced by oxydehydrogenation of propane could be adsorbed on the Brønsted acid sites, and then undergo overoxidation by reaction with one of the redox sites in the neighbourhood. This cooperative effect (presence of Brønsted sites in proximity of agglomerated redox sites) might account for the low selectivity of the V_2O_5/ZrO_2 and V_2O_5/TiO_2 catalysts. This feature should be less effective for V_2O_5/SiO_2 and V_2O_5/Al_2O_3 systems, where the dispersion of active sites is much higher and, in fact, they exhibit a high selectivity towards propene. Though V_2O_5/H–Na/Y catalyst contain highly disperse VO_x species, the presence of a large amount of Brønsted acid protons in its porous structure, where the catalytic active sites are located, results in the low selectivity of this system.

Finally, the poor selectivity of the V_2O_5/MgO catalyst, where Brønsted acid sites were not detected, can be ascribed to the formation of a magnesium vanadate phase active in the total oxidation of propane.

References

[1] H.H. Kung, Adv. Catal. 40 (1994) 1.
[2] E.A. Mamedov, V. Cortés Corberán, Appl. Catal. A 127 (1995) 1.
[3] S. Albonetti, F. Cavani, F. Trifiró, Catal. Rev. Sci. Eng. 38 (1996) 413.
[4] I.E. Wachs, B.M. Wechusyen, Appl. Catal. A 157 (1997) 67.
[5] T. Blasco, J.M. López Nieto, Appl. Catal. A 157 (1997) 117.
[6] B. Grzybowska-Swiekkosz, Appl. Catal. A 157 (1997) 409.
[7] M. Puglisi, F. Arena, F. Frusteri, V. Sokolovskii, A. Parmaliana, Catal. Lett. 41 (1996) 41.
[8] F. Arena, F. Frusteri, G. Martra, S. Coluccia, A. Parmaliana, in: A. Parmaliana, D. Sanfilippo, F. Frusteri, A. Vaccari, F. Arena (Eds.), Proceedings of the Fifth International Gas Conversion Symposium, Vol. 119, Elsevier, Amsterdam, 1998, p. 665.
[9] A. Parmaliana, G. Martra, F. Frusteri, S. Coluccia, F. Arena, submitted for publication.
[10] G. Deo, I.E. Wachs, J. Catal. 146 (1994) 323.
[11] F. Arena, F. Frusteri, G. Martra, S. Coluccia, A. Parmaliana, J. Chem. Soc., Faraday Trans. 93 (1997) 3849.
[12] J.M. López-Nieto, G. Kremenic, J.L.G. Fierro, Appl. Catal. 61 (1990) 235.
[13] S. Coluccia, L. Marchese, G. Martra, Micropor. Mesopor. Mater. 30 (1999) 43, and reference therein.
[14] A. Burneau, J.P. Gallas, in: A.P. Legrand (Ed.), The Surface Properties of Silica, Wiley, Chichester, 1998, p. 147 (Chapter 3A).
[15] C. Morterra, G. Magnacca, Catal. Today 27 (1996) 497.
[16] S. Coluccia, S. Lavagnino, L. Marchese, Mater. Chem. Phys. 18 (1988) 445.
[17] C. Morterra, J. Chem. Soc., Faraday Trans. 84 (1988) 1617.
[18] A.A. Tsygamenko, V.N.F. Filimonov, J. Mol. Struct. 19 (1973) 570.
[19] M. Schraml-Marth, A. Wokaun, M. Pohl, H.-L. Krauss, J. Chem. Soc., Faraday Trans. 87 (1991) 2635.

[20] S. Coluccia, A.J. Tench, R.L. Segall, J. Chem. Soc., Faraday Trans. 1 (75) (1979) 1769.
[21] G. Spoto, C. Morterra, L. Marchese, L. Orio, A. Zecchina, Vacuum 41 (1990) 37 and references therein.
[22] G. Busca, A. Zecchina, Catal. Today 20 (1994) 61, and references therein.
[23] M. Scheithauer, T.-K. Cheung, R.E. Jentoft, R.K. Grasselly, B.C. Gates, H. Knözinger, J. Catal. 180 (1998) 1.
[24] C. Morterra, L. Orio, V. Bolis, P. Ugliengo, Mater. Chem. Phys. 29 (1991) 457.
[25] G. Cerrato, S. Bordiga, S. Barbera, C. Morterra, Surf. Sci. 377–379 (1997) 50.
[26] R.K. Grasselli, in: J. Bonnelle, B. Delmon, E. Derouane (Eds.), Surface Properties and Catalysis by Non-Metals, Reidel, Dordrecht, 1983, p. 273.
[27] G. Busca, L. Marchetti, G. Centi, F. Trifiro', J. Chem. Soc., Faraday Trans. 1 (81) (1985) 1003.
[28] H. Miyata, K. Fuji, T. Ono, J. Chem. Soc., Faraday Trans. 1 (84) (1988) 3121.
[29] R.A. Rajadhyasha, H. Knözinger, Appl. Catal. 51 (1989) 81.
[30] G. Ramis, G. Busca, F. Bregani, P. Forzatti, Appl. Catal. 64 (1990) 259.
[31] N.-Y.H. Topsoe, J.A. Dumesic, J. Catal. 151 (1995) 226.
[32] F. Prinetto, G. Ghiotti, M. Occhiuzzi, V. Indovina, J. Phys. Chem. 102 (1998) 10316.
[33] G. Busca, G. Martra, A. Zecchina (compilers), Catal. Today 56 (2000) 361.
[34] M.A. Chaar, D. Patel, H.H. Kung, J. Catal. 109 (1988) 463.
[35] D. Siew Hew Sam, V. Soenen, J.C. Volta, J. Catal. 123 (1990) 417.